



## (2-Hydroxypropyl)-Beta-Cyclodextrin-hydroxyapatite hybrid compounds prepared by hydrothermal method for environmental applications

H. Agougui<sup>\*1,2</sup>, N. Mabrouki<sup>3</sup>, M. Jabli<sup>4</sup>, K. Boughzala<sup>3</sup>

<sup>1</sup> Laboratory of Physical-chemistry of Materials, Faculty of Sciences of Monastir, 5019 Monastir, Tunisia

<sup>2</sup> Faculty of Sciences of Gafsa, University of Gafsa, University Campus, Zarroug, 2112, Gafsa, Tunisia

<sup>3</sup> Research Unit of Analyzes and Applied Procedures to the Environment, Higher Institute of Applied Sciences and Technology of Mahdia

<sup>4</sup> Textile Materials and Process Research (LMPTEX), National School of Engineering of Monastir (ENIM), Monastir 5000, Tunisia

\*Corresponding author, Email [addresshassenagougui@yahoo.fr](mailto:addresshassenagougui@yahoo.fr)

Received 31 Jan 2022,  
Revised 26 Mar 2022,  
Accepted 28 Mar 2022

### Keywords

- ✓ Hydroxyapatite
- ✓ atomic force microscopy 1,
- ✓ 2-Hydroxypropyl)-β-cyclodextrin .

[hassenagougui@yahoo.fr](mailto:hassenagougui@yahoo.fr)  
Phone: +21654648194;

### Abstract

Hydroxyapatite nanoparticles were prepared in the presence of (2-Hydroxypropyl)-β-cyclodextrin (HP-β-CD) by hydrothermal method at 120 °C for 15 h. The influence of the amount of (HP-β-CD) on the surface of CaHAp was studied. The evidence of interaction was confirmed by FTIR and XRD. The surface topography, the roughness and the morphology of the samples were studied by AFM and SEM. The Chemical analysis proved that the CaHAp nanoparticles could be synthesized using HP-β-CD, in which the Ca/P molar ratio was ranged from 1.72 to 1.70. The crystal size of nanoparticles was found to be decreased with increasing the content of HP-β-CD. The results showed that HP-β-CD could be easily reacted onto the CaHAp surface by forming a Ca-O-C bond between the (≡CaOH) superficial groups of the apatite and hydroxyl groups of HP-β-CD. SEM and AFM showed, respectively, that the morphology of particles and texture surface were changed

## 1. Introduction

Calcium hydroxyapatite,  $\text{Ca}_{10}(\text{PO}_4)_6(\text{OH})_2$  referred as CaHAp, has attracted a particular attention due to its excellent biocompatibility, bioactivity and similarity in chemical composition with human bone tissues [1]. The functionalization of CaHAp with various polymers has been the subject of many studies because they could have the combination properties such as toughness, heat resistance, good thermal, mechanical and adsorption properties. Such hybrid material is used in medical, surgical and environmental applications [2-4]. There are many studies on the interaction between hydroxyapatite and polymers such as polyvinyl alcohol (PVA) [5], poly lactic acid (PLA) [6], Poly acrylic acid (PAA) [7], Poly Vinyl Pyrrolidone (PVP) [8], Dextran [9], and poly(methyl methacrylate) (PMMA) [10]. 2-Hydroxypropyl)-β-cyclodextrin (HP-β-CD) is a polymer belonging to the family of cyclic oligosaccharides with a hydrophilic outer surface and a lipophilic central cavity. It is an important polymer due to its complexation ability. β-CD can form complexes with pesticides, herbicides, insect repellents, etc. Also, in environmental sciences, β-CD is used in the removal of

organic pollutants and heavy metals from water [11]. In our previous works, we have published interesting results about the surface modification of CaHAp using dichlorophosphonate [12] and phosphonic acid [13]. From our results, we have proposed a reaction between the surface “P–O–H” and “Ca–O–H” groups and the phosphonic acid, this reaction leading, to the formation of P–O–P and Ca–O–P bonds. This hybrid compounds can be used for many applications. In line with our interest to apatite functionalized, we carried out a structural, morphological and chemical investigation of CaHAp nanoparticles synthesized by hydrothermal method in the presence of increasing amounts of 2-Hydroxypropyl-Beta-Cyclodextrin (HP- $\beta$ -CD).

## 2. Experimental

### 2.1 Synthesis and functionalization of CaHAp nanoparticles

The synthesis of CaHAp nanoparticles was carried out in aqueous medium using the hydrothermal method [14]. In order to obtain a stoichiometric hydroxyapatite (Ca/P = 1.67), Ca(NO<sub>3</sub>)<sub>2</sub>·4H<sub>2</sub>O solution (15 mL, 0.75 M) was mixed at stirring with (NH<sub>4</sub>)<sub>2</sub>HPO<sub>4</sub> (25 mL, 0.25 M) solution under N<sub>2</sub> bubbling. The pH of the mixture was maintained at 10 with addition of ammonium hydroxide solution (NH<sub>4</sub>OH). The resulting mixture was treated in an autoclave (V= 60 mL) under hydrothermal conditions at 120 °C, for 15 h. After filtration and washing with hot water, the obtained precipitate was dried at 80 °C overnight. The functionalization of CaHAp nanoparticles with HP- $\beta$ -CD was obtained according to the same above procedure except for the calcium solution (0.75 M), it was prepared by mixing HP- $\beta$ -CD with mass percentages m(HP- $\beta$ -CD)/m(calcium): 0%, 5%, 20% and 40%. The new products were CaHAp, CaHAp-(HP- $\beta$ -CD)<sub>5</sub>, CaHAp-(HP- $\beta$ -CD)<sub>20</sub> and CaHAp-(HP- $\beta$ -CD)<sub>40</sub>, respectively.

### 2.2 Characterization techniques

The calcium and phosphorus contents were obtained by ICP-OES on a Horiba jobin yvon modele activa. The chemical analysis of the carbon has been determined according to the Anne method [15]. The IR spectra were recorded on a Bio-Rad FTS FT-IR spectrophotometer as KBr pellets in the 4000-400 cm<sup>-1</sup> region. X-ray powder diffractograms were obtained at room temperature on a PANalyticalX’Pert PRO MPD equipped with copper anticathode tube. The surface morphology was examined by means of atomic force microscopy (AFM) (Veeco Instruments Nanoscope III). The morphological observation of the synthesized samples was undertaken using a Philips Fei Quanta 200 scanning electron microscope, equipped with an Energy Dispersive X-ray analysis system (EDX) for semi quantitative analysis of elements.

## 3. Results and discussion

### 3.1 Elemental analysis

The results of the chemical analysis of the studied materials are summarized in **Table 1**. In the case of unmodified CaHAp, the ratio Ca/P (1.60) is less than (1.67), giving a poorly crystallized non-stoichiometric hydroxyapatite. Contrariwise, the atomic ratios Ca/P for the CaHAp modified by (HP- $\beta$ -CD) are near to the stoichiometric value (1.67). The incorporation of HP- $\beta$ -CD polymer in to apatite structure is proved by the total carbon analysis, showing the increasing amount of the total carbon in the solid (**Table 1**). Moreover, the presence of carbon is mainly attributed to the -CH and -CH<sub>2</sub> fragments of HP- $\beta$ -CD polymer. The results of the chemical analysis indicated the obtaining of new organic-inorganic hybrid compounds.

**Table 1.** Chemical composition ( $\pm 0.02$ ) of hydroxyapatite before and after reaction with HP- $\beta$ -CD.

Samples	%Ca	%P	%C	% Ca/P
CaHAp	34.80	16.83	0.13	1.60
CaHAp-(HP- $\beta$ -CD)5	36.13	16.67	0.57	1.69
CaHAp-(HP- $\beta$ -CD)20	36.64	16.46	0.82	1.70
CaHAp-(HP- $\beta$ -CD)40	35.97	16.31	1.29	1.71

### 3.2 IR spectroscopy

**Figure 1** shows the FT-IR spectra of unmodified CaHAp, CaHAp modified with HP- $\beta$ -CD and the HP- $\beta$ -CD powders.

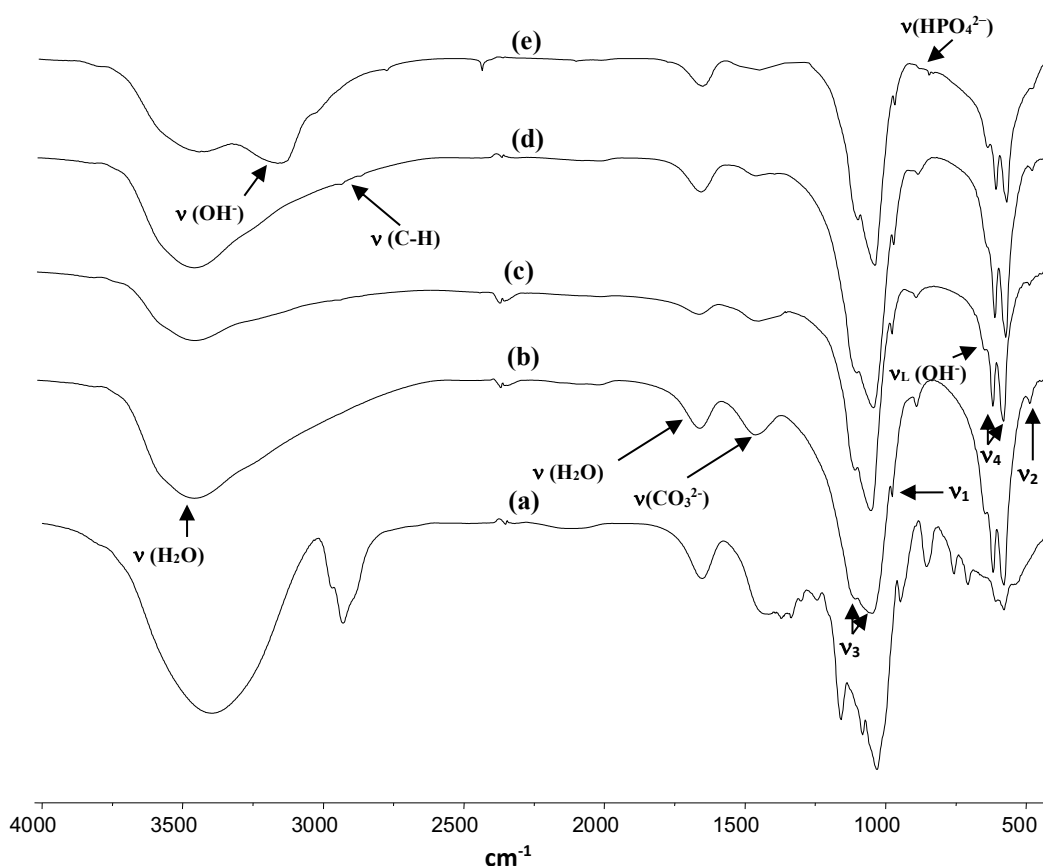


**Figure 1.** IR spectra of: HP- $\beta$ -CD (a); CaHAp(b); CaHAp-(HP- $\beta$ -CD)5 (c); CaHAp-(HP- $\beta$ -CD)20 (d) and CaHAp-(HP- $\beta$ -CD)40 (e).

The IR bands at ( $960\text{ cm}^{-1}$ ), ( $467\text{ cm}^{-1}$ ), ( $1039\text{-}1097\text{ cm}^{-1}$ ) and ( $566\text{-}605\text{ cm}^{-1}$ ) are attributable, respectively, to the  $\nu_1$ ,  $\nu_2$ ,  $\nu_3$  and  $\nu_4$  of  $\text{PO}_4^{3-}$  groups of the apatite structure. For characteristic bands of hydroxyl ions, only ( $\nu_L$ ) at  $630\text{ cm}^{-1}$  is observed. This is due to the decrease in crystallinity. The FT-IR spectrum of CaHAp exhibited bands originating from  $\text{CO}_3^{2-}$  at the wave number range of  $1403\text{-}1462\text{ cm}^{-1}$ . After surface modification, new vibrations bands appear at  $2850$  and  $2950\text{ cm}^{-1}$  which are assigned to C-H and  $\text{CH}_2$  groups of HP- $\beta$ -CD. The IR spectrum of CaHAp-(HP- $\beta$ -CD)40 [Figure 1 (e)] is characterized by an intense band at  $3146\text{ cm}^{-1}$  related to O-H stretching vibration of polymer. Additionally, the relative intensity of characteristic band of ( $\text{HPO}_4^{2-}$ ) at  $875\text{ cm}^{-1}$  decreases

progressively with the increase of the amount of the incorporation of HP- $\beta$ -CD. This decrease could be explained by the possibility the interaction between hydroxyapatite and (HP- $\beta$ -CD) by the  $\equiv$  P-OH groups of apatitic surface and O-H groups of the polymer.

### 3.3 X-ray diffraction

XRD patterns of the modified CaHAp compared to the starting hydroxyapatite, reveal that the apatite structure is not changed (**Figure 2**). These X-ray diffraction patterns indicates the presence of all the diffraction peaks associated to hydroxyapatite of hexagonal system and space group  $P6_3/m$  according to 00-024-0033 reference from the ICDD-PDF2 2003 database. The crystallite sizes ( $D$ ) of all prepared samples were estimated from XRD results by the Debye–Scherrer equation [16]:

$$D = \frac{K\lambda}{\beta_{1/2} \cos \theta}$$

where  $D$  is the crystallite size, as calculated for the (hkl) reflection,  $\lambda$  is the wavelength,  $\theta$  is the diffraction angle,  $K$  is a fixed constant equal to 0.9 for apatite crystallites.

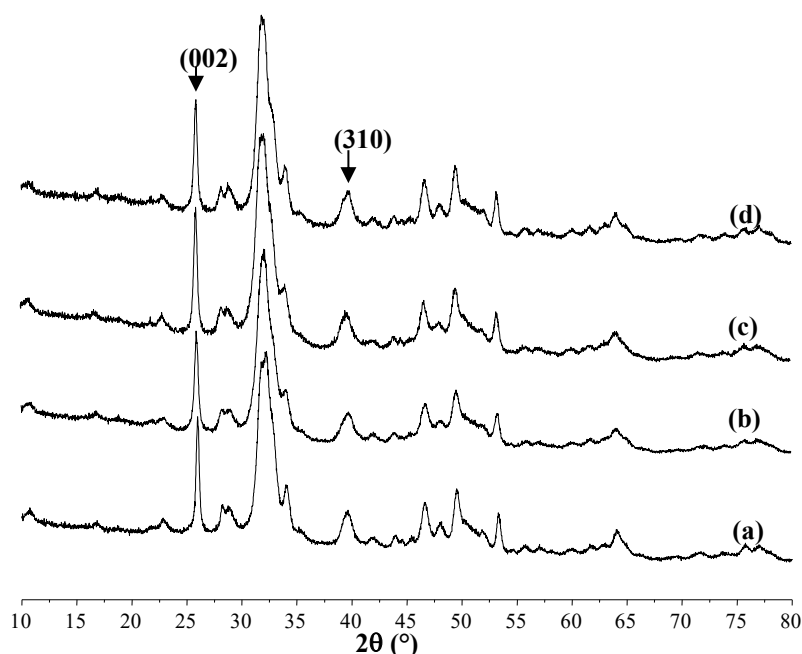


**Figure 2.** X-ray powder diffraction pattern of CaHAp before and after treated by HP- $\beta$ -CD: CaHAp(a); CaHAp-(HP- $\beta$ -CD)5 (b); CaHAp-(HP- $\beta$ -CD)20 (c) and CaHAp-(HP- $\beta$ -CD)40 (d).

The values of full width at half ( $\beta_{1/2}$ ) for the (002) and (310) reflection peaks were used to calculate the crystallite sizes along the  $c$  and  $a$  axes, respectively. The **Table 2** lists the XRD data and crystallite sizes of the products along the directions (002) and (310). The decrease in  $D_{002}$  and  $D_{310}$  values with increasing the amount of polymer, shows that the crystallite size is affected by the presence of HP- $\beta$ -CD. According to **Table 2**, the decrease of crystalline growth is more important along the (002) direction, suggesting a strong interaction between the HP- $\beta$ -CD and hydroxyapatite in this direction. The effect of HP- $\beta$ -CD polymer treatment on CaHAp crystallinity was evaluated by the following formula [17]:

$$X_c = \left( \frac{K_A}{\beta_{1/2}} \right)^3$$

Where KA is a constant set at 0.24 and  $\beta_{1/2}$  is the FWHM of the (0 0 2) reflections. The estimated crystallinity ( $X_c$ ) data of all compounds are given in **Table 3**. According to the  $X_c$  values, the crystallinity degree decreases progressively with the increase of the amount of HP- $\beta$ -CD incorporated onto the hydroxyapatite surface. The lattice parameters of all synthesized materials were determined using the EXPO 2009 software [18]. Table 3 shows that the a and c parameters varied slightly, when the rate of the incorporated polymer increases into the starting solution.

**Table 3.** The lattice parameters of hydroxyapatites before and after modifying by (HP- $\beta$ -CD).

Sample	a (Å)	c (Å)
CaHAp	9.418	6.865
CaHAp-(HP- $\beta$ -CD)5	9.421	6.869
CaHAp-(HP- $\beta$ -CD)20	9.428	6.885
CaHAp-(HP- $\beta$ -CD)40	9.433	6.883

### 3.4 Solid state NMR spectroscopy

$^{31}\text{P}$  MAS-NMR spectra of CaHAp before and after modifying by HP- $\beta$ -CD are given in **Figure 3**. An isotropic signal appears at 2.51 ppm in unmodified CaHAp (**Figure 3a**). After the addition of HP- $\beta$ -CD and an increase in HP- $\beta$ -CD concentration, the  $^{31}\text{P}$  characteristic signal moves to 2.78 ppm as shown in **Table 4**.

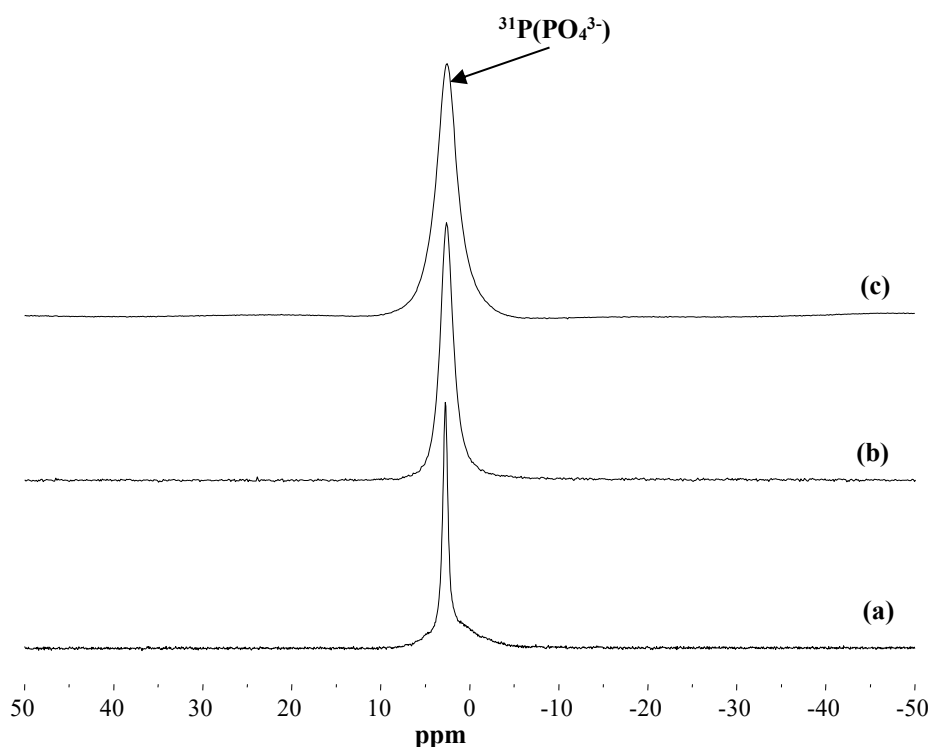


**Figure 3.**  $^{31}\text{P}$  CP/MAS-NMR spectra of CaHAp before and after grafting (HP- $\beta$ -CD): unmodified (a); CaHAp-(HP- $\beta$ -CD)20(b) and CaHAp-(HP- $\beta$ -CD)40 (c).

In fact, this shift is due to the interaction of CaHAp with HP- $\beta$ -CD leading to the formation of CaHAp-HP- $\beta$ -CD. In addition, the treatment of hydroxyapatite leads to a significant broadening of the

isotropic signal (Table 4). These results indicate that after the formation of hybrid compounds, the chemical environment of the phosphorus atom in solid phase has been changed [19]. This shows that the chemical interaction between HP- $\beta$ -CD and CaHAp surface may be due to the interaction between the OH groups belonging to HP- $\beta$ -CD and the constituents of apatitic surface ( $\equiv$ Ca-OH and  $\equiv$ POH).

**Table 4.** Chemical shifts of CaHAp before and after reaction with (HP- $\beta$ -CD).

Samples	$\delta_{\text{iso}} \pm 0.1(\text{ppm})$	$\Delta_{1/2}$
CaHAp	2.51	0.77
CaHAp-(HP- $\beta$ -CD)20	2.63	1.59
CaHAp-(HP- $\beta$ -CD)40	2.78	2.47

### 3.5 SEM observation and EDX analysis

The analysis SEM was conducted on all samples in order to investigate the effects of (HP- $\beta$ -CD) on CaHAp morphology during the modifying process. Figure 4 shows the morphological variations of CaHAp before and after reaction with HP- $\beta$ -CD. The CaHAp is composed of irregular particles, with a strong tendency to aggregate (figure 4a), whereas the sample prepared in the presence of HP- $\beta$ -CD showed, that their shapes become relatively agglomerates of different sizes and poorly defined shape (figures 4(b-d)).

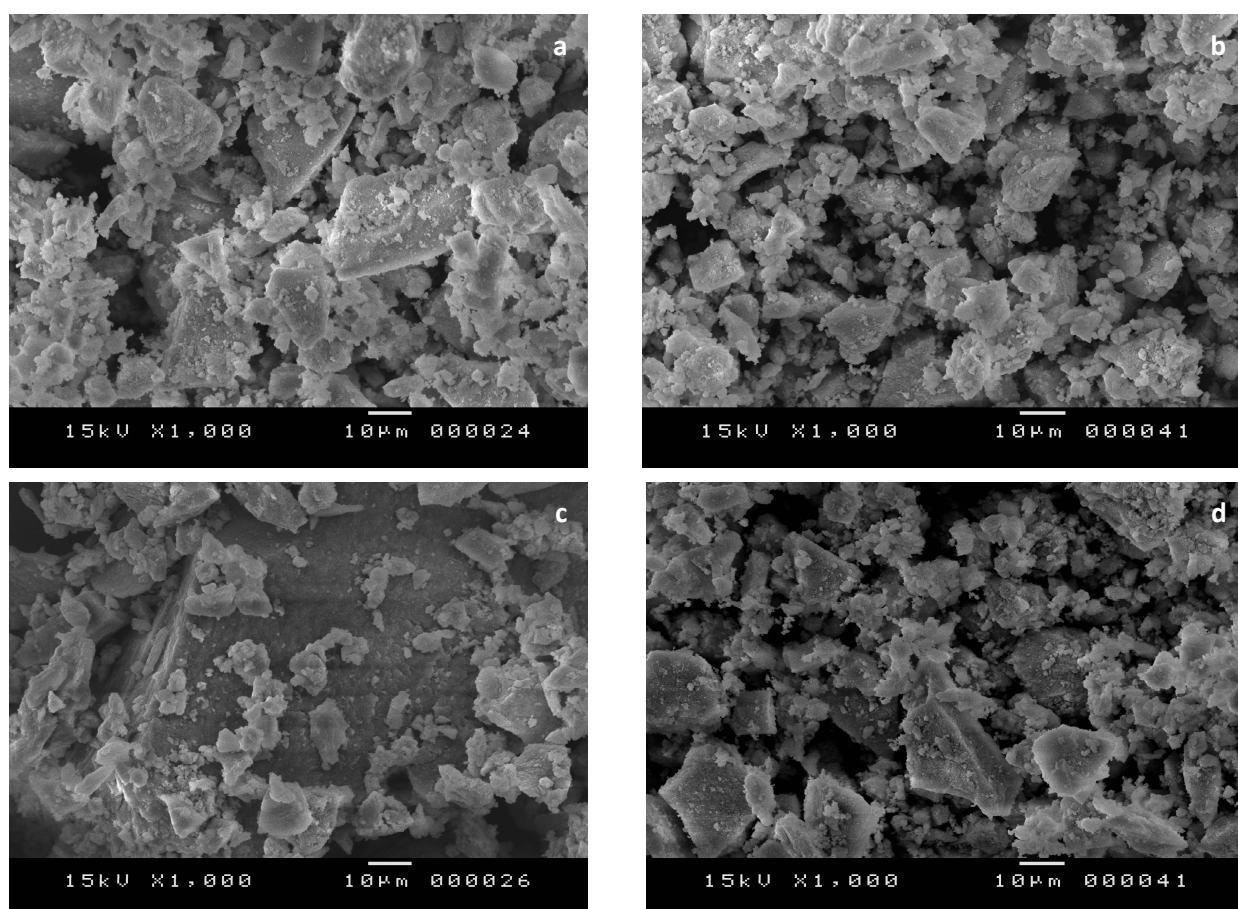


**Figure 4.** SEM images of (a) unmodified, (b) CaHAp-(HP- $\beta$ -CD)5, (c) CaHAp-(HP- $\beta$ -CD)20 and (d) CaHAp-(HP- $\beta$ -CD)40.

EDX analysis (**Figure 5**) of treated CaHAp by HP- $\beta$ -CD confirmed the presence of Ca, P, O and C by showing characteristic peaks of unmodified CaHAp. On the other hand, the peak intensity of carbon becomes more intense when the rate of incorporated HP- $\beta$ -CD increases. These results are in good agreement with those obtained previously in the part of X-ray diffraction.

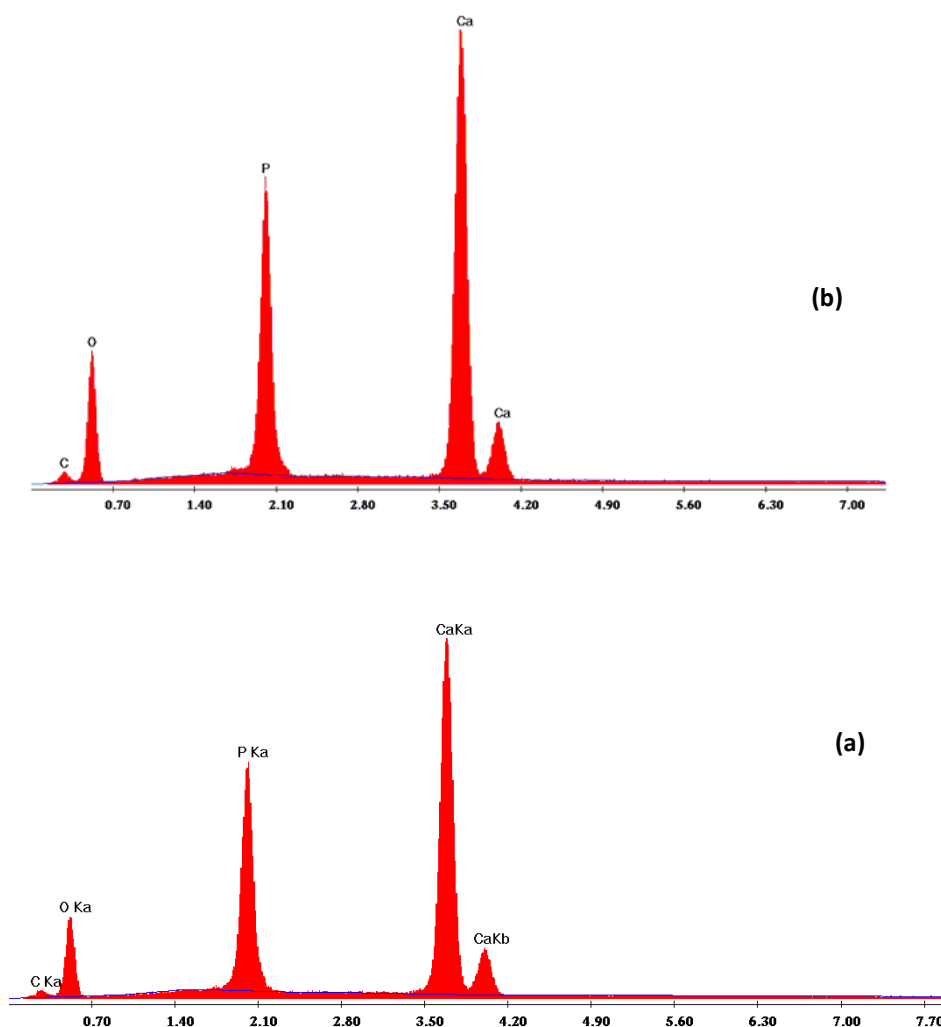


**Figure 5.** EDX spectrum of (a) CaHAp and (b) CaHAp-(HP- $\beta$ -CD)20.

### 3.5 Study by Atomic Force Microscopy (AFM)

A selection of (3D) and (2D) AFM images of the hydroxyapatite modified with HP- $\beta$ -CD is presented in **Figure 6**. The AFM images show that samples exhibit a different surface topography. The surface roughness (RMS) of CaHAp is 260 nm. The increase in the HP- $\beta$ -CD composition that is 20 wt%, leads to a decrease from the surface roughness up to 50 nm. This change is due to the interaction of CaHAp with HP- $\beta$ -CD in CaHAp/HP- $\beta$ -CD hybrid compound.

In 3-D topographic image for CaHAp before and after unmodified by HP- $\beta$ -CD (**Figure 6**) can be seen on the grain growth in direction z. The AFM showed that the particle growth process was blocked by HP- $\beta$ -CD polymer introduced in synthesis, which is adsorbed on the surface of particles and stops the further growth of particles. This result is in good agreement with the decrease of the crystallinity degree and the crystallites size in the XRD patterns.

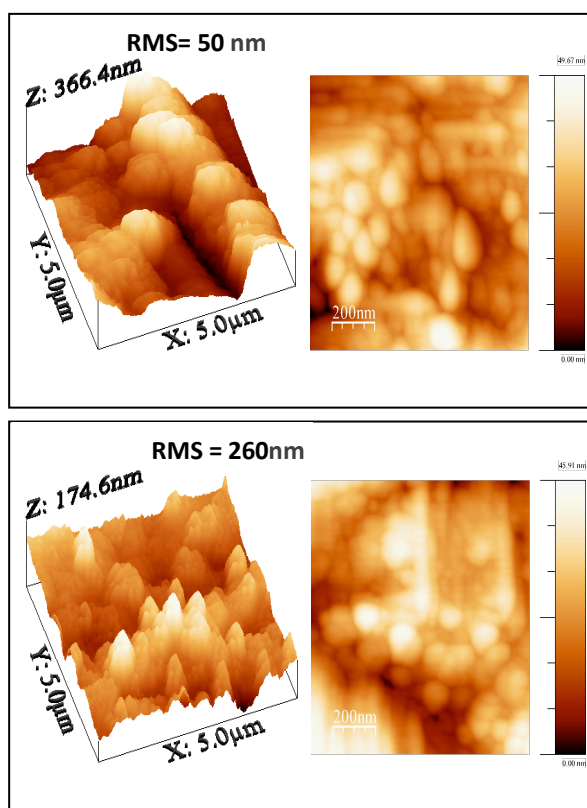


**Figure 6.** Three-dimensional (3D) and two-dimensional (2D) images of atomic force microscopy (AFM) of modified CaHAp: (a) CaHAp and (b) CaHAp-(HP- $\beta$ -CD)20.

## Conclusion

In this study, HP- $\beta$ -CD/CaHAp hybrid compounds have been successfully synthesized using hydrothermal method. FTIR result of these novel compounds suggest the presence of functional groups like(C-H) and (O-H) of HP- $\beta$ -CD in apatitic phase. The SEM investigations revealed that there is a distribution of small particles and large agglomerates with an irregular morphology. XRD diffraction and AFM results indicate that the HP- $\beta$ -CD polymer is extremely effective to inhibit CaHAp crystal growth. Therefore, all characterization techniques show that the incorporation of HP- $\beta$ -CD on the surface of CaHAp is bonded by interaction between constituents of apatitic surface ( $\equiv$ Ca-OH and  $\equiv$ POH) and OH groups of HP- $\beta$ -CD polymer. Further work could be extended to check these developed HP- $\beta$ -CD/CaHAp hybrid compounds in environmental applications, including the removal of different types of dyes and heavy metal ions from wastewater.

## Acknowledgement

The authors thank the Institut Nationale de Recherche et d'Analyses Physico-Chimiques, Institut Nationale de Recherche Scientifique et Technologique, the Company of Phosphate Gafsa and the University of Monastir (Tunisia).

**Disclosure statement:** *Conflict of Interest:* The authors declare that there are no conflicts of interest. *Compliance with Ethical Standards:* This article does not contain any studies involving human or animal subjects.

## References

- [1] E. Fiume, G. Magnaterra, A. Rahdar, E. Verné and F. Baino, "Hydroxyapatite for Biomedical Applications: A Short Overview , " *Ceramics*, 4 (2021) 542-563.
- [2] E.M. Abdelrazek, A.M. Hezma, N. El-sheshtawy, S. Elbeltagy and A. El-Khodary, " Investigating the effect of incorporating nanosilver/nanohydroxyapatite with blend of (PAAc-Cs) on the shear bond strength of human bone, " *Res. J. Pharm. Biol. Chem. Sci*, 5(6) (2014) 1267.
- [3] T. V. katesan, R. Vinayagam, S. Pai, K. Brindhadevi, A. Pugazhendhi, R. Selvaraj, " Synthesis, biological and environmental applications of hydroxyapatite and its composites with organic and inorganic coatings, " *Progress in Organic Coatings*, 151 (2021) 106056.
- [4] A. Lamhamdi, K. Azzaoui, E. Mejdoubi, B. Hammouti, M. Berrabah, M. Zegmout, B. Razzouki, " Contribution of adsorption of metals using calcium phosphates in the presence of support polyethylene glyco, " *Journal of Materials and Environmental Science*, 5(S2) (2014) 2584-2589.
- [5] T.V. Safronova, M.A. Shekhirev, V.I. Putlyayev, " Ceramics Based on Calcium Hydroxyapatite Synthesized in the Presence of PVA, " *Glass and Ceramics*, 64 (2007) 408-412.
- [6] J. Russias, E. Saiz, R.K. Nalla, K. Gryn, R.O. Ritchie, A.P. Tomsia, " Fabrication and mechanical properties of PLA/HA composites: A study of in vitro degradation" *Materials Science and Engineering: C*, 26 (2006) 1289-1295.
- [7] E. Bertoni, A. Bigi, G. Falini, S. Panzavolta, N. Roveri, " Hydroxyapatite/polyacrylic acid nanocrystals, " *Journal of Materials Chemistry*, 9 (1999) 779-782.
- [8] A. Ragu, K. Senthilarasan, P. Sakthivel, " Synthesis and characterization of nano hydroxyapatite with poly vinyl pyrrolidone nano composite for bone tissue regeneration , " *International journal of engineering research and applications*, 4 (7) (2014) 50-54.
- [9] A. Costescu, E. Andronescu, B. Ștefan Vasile, R. Trușcă, P. le coustumer, E. Ștefan Barna, S. Liliana Iconaru, M. Motelica-Heino, C. Steluța Ciobanu, " Thermoelectric power in liquid compositions richer in s than tl2s semiconductor compound, " *U.P.B. Scientific Bulletin Series B*, 76 (4) (2014) 1454-2331.
- [10] A. Balamurugan, S. Kannan, V. Selvaraj, S. Rajeswari, " Development and spectral characterization of poly(methyl methacrylate)/hydroxyapatite composite for biomedical applications , " *Trends in Biomaterials & Artificial Organs*, 18(1) (2004) 41-45.
- [11] S. Fourmentin, D. Landy, P. Blach, E. Piat, G. Surpateanu, Cyclodextrins: A potential absorbent for VOC abatement, *Global Nest Journal*, 8(3) (2006) 324-329.
- [12] A. Aissa, M. Debbabi, M. Gruselle, R. Thouvenot, P. Gredin, R. Traksmaa, "K.Tönsuaadu, Covalent modification of calcium hydroxyapatite surface by grafting phenyl phosphonate moieties , *Journal of Solid State Chemistry*, 180 (2007) 2273-2278.
- [13] M. Othmani, A. Aissa, A. Grelard, R.K. Das, M. Debbabi, R. Oda, Synthesis and characterization of hydroxyapatite-based nanocomposites by the functionalization of hydroxyapatite nanoparticles with phosphonic acids, *Colloids and Surfaces A: Physicochemical and Engineering Aspects*, 508 (2016) 336-344.
- [14] H. Agougui, A. Aissa, S. Maggi, M. Debbabi, " Synthesis of hydroxyapatite-sodium alginate via a co-precipitation technique for efficient adsorption of Methylene Blue dye, " *Applied Surface Science*, 257 (2010) 1377-1382.
- [15] P. Anne, " Sur le dosage rapide du carbone organique des sols, " *Annales Agronomiques*, 15 (1945) 161-172.

- [16] S. Sibte Asghar Abidi, Q. Murtaza, " Synthesis and Characterization of Nano-hydroxyapatite Powder Using Wet Chemical Precipitation Reaction, " *International Journal of Molecular Sciences*, 30 (4) (2014) 307-310.
- [17] J. Kolmas, M. Kuras, E. Oledzka and M. Sobczak, " A Solid-State NMR Study of Selenium Substitution into Nanocrystalline Hydroxyapatite, " *International Journal of Molecular Sciences* , 16 (2015) 11452–11464.
- [18] A. Altomare, M. Camalli, C. Cuocci, C. Giacovazzo, A. Moliterni, R. Rizzi, "EXPO2009: Structure solution by powder data in direct and reciprocal space" *Journal of Applied Crystallography*, 42 (2009) 1197-1202.
- [19] T. Turki, M. Othmani, J.L. Bantignies, K. Bouzouita, "Hydroxyapatite-phosphonoformic acid hybrid compounds prepared by hydrothermal method" *Applied Surface Science*, 292 (2014) 327-331.